



Recent Advances In Nano Science And Technology 2015 (RAINSAT2015)

## MnO<sub>2</sub>-Vertical graphene nanosheets composite electrodes for energy storage devices

Subrata Ghosh\*, Bhavana Gupta, K. Ganesan, A. Das, M. Kamruddin, S. Dash, A.K. Tyagi

*Surface & Nanoscience Division, Materials Science Group, Indira Gandhi Centre for Atomic Research, Tamil Nadu, India - 603102*

---

### Abstract

The vertical graphene nanosheets (VGNs) have attracted considerable attention for energy storage application due to their inherent properties such as morphology, large surface area, high electrical conductivity and three dimensional (3D) open network structures. Here, we report on the growth of VGNs using electron cyclotron resonance - chemical vapor deposition and its electrochemical storage behavior. Further, a near homogeneous dispersion of MnO<sub>2</sub> is coated over VGNs by dip casting to enhance the effective capacitance. Electrochemical charge storage behavior of VGNs and MnO<sub>2</sub>/VGNs composites are investigated using cyclic voltametry and electrochemical impedance spectroscopy (EIS) and also the results are compared. The MnO<sub>2</sub>/VGNs composites exhibit the highest areal capacitance of 5.6 mF/cm<sup>2</sup>, which is 110 times higher than that of VGNs (51.95 μF/cm<sup>2</sup>) at a scan rate of 50 mV/s. The enhanced capacitance is due to highly conductive 3D network of VGNs which provide fast electron and ion transport and also a large pseudo-capacitance from MnO<sub>2</sub> coating. The EIS results are analyzed with equivalent circuit model which reveals the charge storage mechanism in the materials. Scanning electron microscopy and Raman spectroscopy are also used to understand the morphology and structure – property correlations of the films. These results demonstrate clearly that the MnO<sub>2</sub>/VGNs composite is a potential candidate for energy storage applications.

© 2015 Elsevier Ltd. All rights reserved.

Selection and Peer-review under responsibility of [Conference Committee Members of Recent Advances In Nano Science and Technology 2015].

*Keywords:* vertical graphene nanosheets; MnO<sub>2</sub>; energy storage; impedance spectroscopy

---

\* Corresponding author. Tel.: Tel.: +91-44-27480500-22791

*E-mail address:* [subrataghosh.phys@gmail.com](mailto:subrataghosh.phys@gmail.com)

## 1. Introduction

The energy storage and efficient energy delivery are among the emerging fields being contemplated for academic and industrial research. In this aspect, supercapacitors (SCs) have drawn tremendous interest due to their high power density, long life cycle and low maintenance costs [1]. The selection of suitable electrode material with increased energy density has been the biggest challenge in energy storage devices of this century. An ideal material should have high electrolyte accessible network along with high electrical conductivity, good mechanical and chemical stabilities. To date, carbon nanostructured materials, transition-metal oxides (TMOs) and conducting polymers have been extensively used as active electrode materials for charge storage applications [2-5]. Among others, carbon nanostructured materials with high surface area demonstrate high mechanical performance, chemical stability and high electrical conductivity but they possess poor capacitance. On the other hand, TMOs show high capacitance and fast redox kinetics, despite having poor electrical conductivity, high charge-transfer resistance and low structural stability. In this context, a lot of scientific research has been focused towards development of carbon nanostructures –TMOs hybrid materials. Such hybrid materials can combine the advantages of both the types of materials.

The vertical graphene nanosheet (VGNs), one of the beneficial architectural engineering of graphene, has attracted significant attention for the energy storage applications due to its unique morphology, high surface area, excellent electrical conductivity and open network structure. The VGNs consist of vertically aligned graphene nanosheets which are freely standing perpendicular to the substrates.[6-11] Each sheet is composed of a few layers of graphene with length and height ranging from a few nanometers to microns. Thus, the VGNs have many advantages like providing conductive path for fast electron transport and the porous structures which help to increase the ion transport area and also large surface area for designing hybrid structures. These properties help VGNs to have high specific capacitance and the reported values are found to be as high as 50–70  $\mu\text{F}/\text{cm}^2$  [7]. It is also reported that the areal specific capacitance of edge planes is much higher than that of the basal plane graphene electrodes (3  $\mu\text{F}/\text{cm}^2$ ) [6]. Miller et al [6] are demonstrated efficient ac line-filtering performance with double layer capacitance based on VGNs electrodes. The VGNs are generally grown on different electrically conducting substrates like carbon paper, glassy carbon, Ni or Ni foam and those conducting substrates which act as current collector in storage devices [6-10]. Since the VGNs grow always with a high conductive nanographitic base layer, one can utilise the nanographite base layer itself as a current collector for working electrode which is not reported earlier. Furthermore, a few groups have shown the energy storage performance of MnO<sub>2</sub>/VGNs composites [8,9]. But, the electrochemical impedance study to explore the charge storage mechanism of VGNs and MnO<sub>2</sub>/VGNs composites are scarce. Herein, we report on efficient energy storage performance of VGNs that are directly grown on n-Si(100) and its hybrid electrode materials. The charge storage mechanism is also analysed using electrochemical impedance spectroscopy (EIS). These studies reveal that MnO<sub>2</sub>/VGNs composites can be an alternative active electrode material for energy storage devices.

## 2. Experimental methods

### 2.1. Growth of vertical graphene nanosheets

The VGNs are grown by electron cyclotron resonance chemical vapor deposition with CH<sub>4</sub>/Ar plasma. The details of the experiment can be found elsewhere [11]. Prior to deposition, the substrates are pre-cleaned by Ar plasma with 20 sccm flow for 10 min at 200 W power. Thereafter, CH<sub>4</sub> of 5 sccm is fed into the chamber along with Ar gas of 35 sccm at microwave power of 400W and temperature of 800°C over duration of 2 hrs. After the growth, the plasma is turned off and the samples are annealed at the same temperature for 30 minutes. Subsequently, the samples are allowed to cool naturally to room temperature.

## 2.2. Deposition of $MnO_2$

The VGNs on *n*-Si(100) is dipped into 10 mM  $KMnO_4$  acidic aqueous solution and kept at 60°C for 2 minutes to incorporate  $MnO_2$  [12]. As prepared electrode is washed in deionized water and dried in open atmosphere for 30 min. Without any binder  $MnO_2$ /VGNs electrode is prepared.

## 2.3. Structural and electrochemical characterization

The morphology of deposited films is observed by a field emission scanning electron microscope (FESEM, Supra 55, M/s Zeiss). The structural properties are investigated by Raman spectroscopy (inVia, M/s Renishaw) with 514.5 nm laser wavelength and 100× objective lens. In order to avoid the laser induced heating on the sample, the laser power is kept below 1 mW.

The cyclic voltammetry (CV) and EIS studies are carried out using Potentiostat/Galvanostat (M/s Metrohm-Autolab, The Netherlands). The studied materials (graphene and its derivatives) are used as working electrodes where as Ag/AgCl saturated in KCl and platinum mesh act as reference and counter electrodes, respectively. The electrochemical measurements are performed in 0.5 M  $Na_2SO_4$  electrolyte at room temperature. The CV measurements are carried out within the potential range of 0.2-0.8 V against Ag/AgCl at scan rates of 20-200  $mVs^{-1}$ . The EIS is carried out at open circuit potential in the frequency range of 0.1 Hz to 10 kHz. The equivalent circuit analysis is performed using EIS spectrum analyzer software.

## 3. Results and discussion

### 3.1 Morphological analysis

Fig. 1(a-b) shows SEM micrographs of VGNs grown on *n*-Si(100) at different magnifications. These micrographs reveal the interconnected porous network of very thin sheets of graphene. The thickness of each sheet is 3-5 nm and length varies upto a few micrometers. Fig. 1(c) shows the cross sectional SEM micrograph of VGNs on the Si substrates. This image shows that VGNs are standing perpendicular to the substrate.

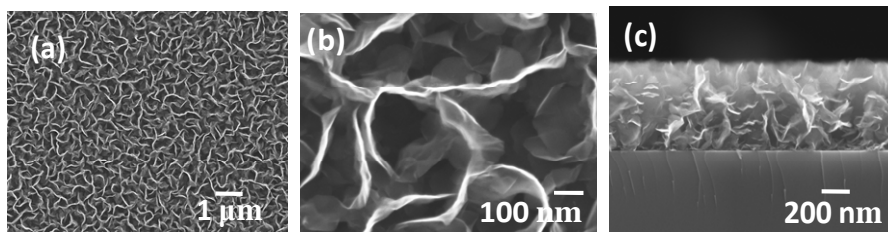


Fig. 1. SEM micrograph of (a) vertical graphene nanosheets (VGNs); (b) VGNs at higher magnification (c) cross section view of VGNs on Si

### 3.2 Raman analysis

Raman spectroscopy is extensively utilized to characterize carbon based materials for their crystallinity and bonding environment [11,13-15]. Fig. 2 illustrates Raman spectra of VGNs and  $MnO_2$ /VGNs. It is observed that Raman spectra of VGNs and  $MnO_2$ /VGNs predominantly consists of graphitic peaks (G- and G'- bands) and defect related bands (D, D', D+D', D+D'' and 2D') [11,13,15]. The position and full width at half maximum (FWHM) are derived from Raman bands of studied materials by Lorentzian line shape analysis and these parameters are given in table 1. The strong D- band in VGNs arises due to the presence of high edge densities and vacancy-like defects [11] The decoration of  $MnO_2$  on VGNs does not show any significant variation in the Raman spectra except a minute broadening of the D-, G- and G'- bands and a new Raman band at  $652.0\text{ cm}^{-1}$  which confirms the presence of  $MnO_2$

layer over VGNs. The FWHM of the Raman band is found to be  $26.3 \text{ cm}^{-1}$  indicating the excellent structural quality of the  $\text{MnO}_2$  layers.

Table 1. The extracted parameters of Raman analysis of VGNs and  $\text{MnO}_2/\text{VGNs}$ .

Materials	D-band		G-band		G'-band		MnO <sub>2</sub>	
	Position	FWHM	Position	FWHM	Position	FWHM	Position	FWHM
VGNs	1353.7	37.7	1583.5	36.0	2701.8	69.42	-	-
$\text{MnO}_2/\text{VGNs}$	1355.6	42.2	1585.3	38.8	2705.2	75.16	652.0	26.3

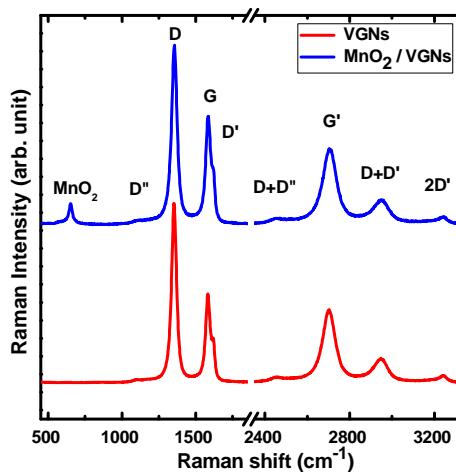


Fig. 2. Raman spectra of VGNs and  $\text{MnO}_2/\text{VGNs}$ .

### 3.3 Electrochemical analysis

#### 3.3.1 CV analysis

Fig. 3(a-b) represents the comparative CV curves of VGNs and  $\text{MnO}_2/\text{VGNs}$  acquired at different scan rates of 20 - 500 mV/s respectively. The nearly rectangular and symmetric CV curves of VGNs and  $\text{MnO}_2/\text{VGNs}$  ensure the highly capacitive behaviour accompanied with good ion diffusivity. The capacitive behaviour of  $\text{MnO}_2/\text{VGNs}$  is a combined effects which arise from electric double layer capacitance (EDLC) of VGNs and pseudocapacitance of  $\text{MnO}_2$ . The areal specific capacitance of electrode materials are calculated from CV curve using the formula given below

$$C_s = \frac{\int I dV}{s \cdot A \cdot \Delta V} \quad (1)$$

where  $C_s$  is areal specific capacitance (in  $\text{F}/\text{cm}^2$ ),  $I$  is the current,  $s$  is scan rate for particular curve,  $A$  is area exposed to electrolyte and  $\Delta V$  is potential window through which active material electrode is scanned. The variation in specific capacitance with respect to scan rate for VGNs and  $\text{MnO}_2/\text{VGNs}$  are listed in table 2. The areal specific capacitance for VGNs is found to be  $51.95 \mu\text{F}/\text{cm}^2$ , which is in good agreement with existing report [6]. From table 2, it is clear that  $\text{MnO}_2/\text{VGNs}$  show a drastically enhanced charge storage capacity over the VGNs. For VGNs, the nanographitic base layer, which forms just before the onset of VGNs growth, acts as current collector. The interconnected uniform porous network of a few layer graphene sheets provide accessibility to large amount of electrolyte ions on its internal surface area which eventually brings better charge storage capacity to the film. On

the other hand,  $\text{MnO}_2/\text{VGNs}$  composite demonstrates about 110 times higher charge storage capacity than the VGNs. The enhancement in charge storage comes from the pseudo-capacitance of  $\text{MnO}_2$  layers coated over a large surface area of VGNs.

Table 2. The areal specific capacitance of VGNs and  $\text{MnO}_2/\text{VGNs}$  at different scan rate as calculated from C-V curve.

Scan rate ( $\text{mVs}^{-1}$ )	Areal sp. capacitance ( $\mu\text{F}/\text{cm}^2$ )	
	VGNs	$\text{MnO}_2/\text{VGNs}$
20	69.42	7364.66
50	51.95	5615.73
100	49.52	4176.6
200	41.07	2749.8
500	35.82	1124.03

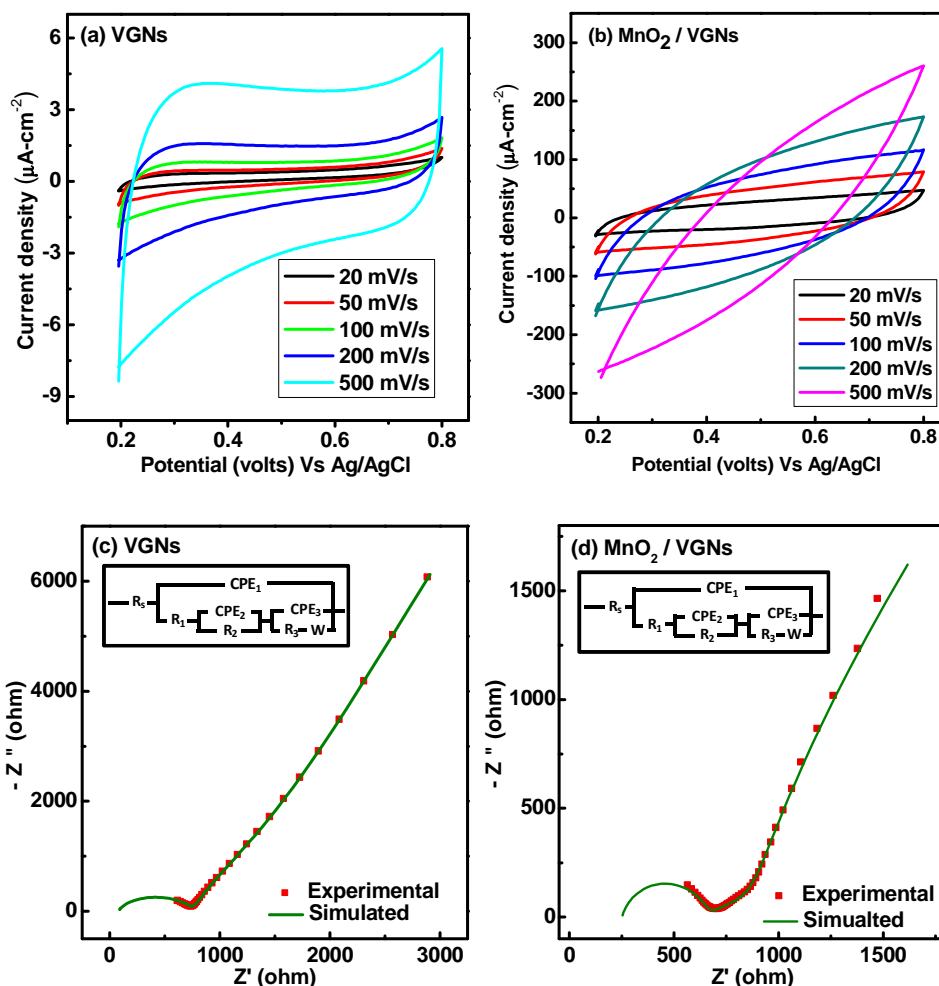


Fig. 3. Electrochemical performance of VGNs and  $\text{MnO}_2/\text{VGNs}$ . CV curves of (a) VGNs and (b)  $\text{MnO}_2/\text{VGNs}$  at a different scan rate of 20 - 500  $\text{mV s}^{-1}$ ; Nyquist plots of (c) VGNs and (d)  $\text{MnO}_2/\text{VGNs}$  measured at 0.5 M  $\text{Na}_2\text{SO}_4$  electrolyte. The inset of fig. 3(c-d) represents the corresponding equivalent circuit

### 3.3.2 EIS analysis

The impedance spectra of VGNs and MnO<sub>2</sub>/VGNs with simulation are shown in Fig. 3(c-d). The Nyquist plots of VGNs and MnO<sub>2</sub>/VGNs show suppressed and normal semicircles with different slopes respectively. To gain deep insight into the behaviour of electrode materials, the impedance spectra are fitted with an equivalent circuit model, as shown in the inset of Fig.3(c-d) [1,16]. The extracted parameters of equivalent circuit are listed in table 3. The equivalent circuits are composed of one resistor element ( $R_s$ ) and three time constants circuits in which one circuit contains Warburg elements.  $R_s$  is series resistance of the electrolyte and charge barriers between current collector and electrode. The highly conductive graphene networks make the  $R_s$  to be low (63.35 ohms) in VGNs whereas the poor conductive MnO<sub>2</sub> layers offers high resistance  $R_s$  in the MnO<sub>2</sub>/VGNs electrode (250.1 ohms) The first component ( $CPE_1$ ,  $n_1$ ,  $R_1$ ) represents the interaction between edges of the graphene sheets and electrolyte ions. No significant change in  $CPE_1$  is observed for both the electrodes. The second component ( $CPE_2$ ,  $n_2$ ,  $R_2$ ) represents the interaction between planar surface of graphene walls and electrolyte ions. The third component ( $CPE_3$ ,  $n_3$ ,  $R_3$ ) represents the interaction between nanographitic base layer and electrolyte ions. In case of MnO<sub>2</sub>/VGNs, a significant increase in capacitive values are observed for  $CPE_2$  and  $CPE_3$  components as compared to VGNs. Similarly, high capacitance is also observed in cyclic voltammetry analysis. The low Warburg impedance ( $W$ ) and high  $n_3$  value are observed for the MnO<sub>2</sub>/VGNs electrode. This result indicates that the MnO<sub>2</sub> entity in this case infiltrates porous architecture of VGNs side walls. The porous structure of VGNs attracts a large amount of MnO<sub>2</sub> which offers better charge transport, and shorten diffusion path for intercalation/deintercalation of active species. Incidentally  $n_3$  value of VGNs and MnO<sub>2</sub>/VGNs is close to 1 representing ideal capacitive behaviour of the electrodes. These results demonstrate improved charge storage capacity of MnO<sub>2</sub>/VGNs than the VGNs electrode.

The pore structure of VGNs provides access of electrolytes over a large surface area. The high structural quality and stable nano-graphitic base layer of VGNs allow higher rates of ions and electrons to transport in electrode. Thus incorporation of MnO<sub>2</sub> in VGNs improves pseudo-capacitance. Hence, MnO<sub>2</sub> decoration strongly enhances the overall charge storage capacity of MnO<sub>2</sub>/VGNs composites.

Table 3. The extracted parameters of equivalent circuit analysis for electrochemical impedance spectra using EIS spectrum analyzer.

	VGNs	MnO <sub>2</sub> /VGNs
$R_s$ [ohm]	63.35	250.1
$CPE_1$ [F]	$8.32 \times 10^{-8}$	$6.63 \times 10^{-8}$
$n_1$ [0<n<1]	0.82	0.87
$R_1$ [ohm]	682.36	407.43
$CPE_2$ [F]	$3.97 \times 10^{-5}$	$48.54 \times 10^{-5}$
$n_2$ [0<n<1]	0.74	0.48
$R_2$ [ohm]	925.38	311.88
$CPE_3$ [F]	$1.04 \times 10^{-5}$	$50.0 \times 10^{-5}$
$n_3$ [0<n<1]	0.92	1.0
$R_3$ [ohm]	$7.99 \times 10^{-13}$	116.66
$W$ [Ohm s <sup>-0.5</sup> ]	102000	1937.5

## 4. Conclusion

The electrochemical behavior of verical graphene nanosheets (VGNs) is investigated using cyclic voltammetry and electrochemical impedance spectroscopy. The VGNs provides controlled porous structure and high electrolyte accessible surface area for multiple pathways for ion transport. We demonstrate that the nanographitic base layer of VGNs itself can serve as conductive path for electron transport. It is shown that MnO<sub>2</sub> can be anchored efficiently on to VGNs to enhance the specific capacitance of electrodes. The MnO<sub>2</sub>/VGNs composites exhibits 110 times

higher charge storage capacity than the VGNs. The charge storage mechanism is also discussed with the help of EIS study, which supports the CV data. These results demonstrate clearly that the MnO<sub>2</sub>/VGNs composite is a potential candidate for energy storage applications.

### Acknowledgements

The authors acknowledge Dr. S. Dhara and Dr. R. N. Viswanath, Materials Science Group, IGCAR. One of the authors, B. G., also would like to thank D. S. T., New Delhi, India for Inspire Fellowship Award.

### References

- [1] B.E. Conway, *Electrochemical supercapacitors: Scientific Fundamentals and Technological Applications*, Plenum, New York, (1999).
- [2] L.L. Zhang, X. Zhao, *Chem. Soc. Rev.* 38 (2009) 2520-2531.
- [3] W. Gu, G. Yushin, *Wiley Interdisciplinary Reviews: Energy and Environment* (2013).
- [4] C. Lokhande, D. Dubal, O.-S. Joo, *Current Applied Physics* 11 (2011) 255-270.
- [5] M.E. Abdelhamid, A.P. O'Mullane, G.A. Snook, *RSC Advances* 5 (2015) 11611-11626.
- [6] J. R. Miller, R. Outlaw and B. Holloway, *Science* 329 (2010) 1637-1639.
- [7] D. H. Seo, Z. J. Han, S. Kumar and K. K. Ostrikov, *Advanced Energy Materials* 3 (2013) 1316-1323.
- [8] S. Hassan, M. Suzuki, S. Mori, A.A. El-Moneim, *J. Power Sources* 249 (2014) 21.
- [9] G. Xiong, K. Hembram, R. Reifenberger and T. S. Fisher, *J. Power Sources* 227 (2013) 254-259.
- [10] Z. Bo, S. Mao, Z. Jun Han, K. Cen, J. Chen, K. Ostrikov, *Chem. Soc. Rev.* 44 (2015) 2018-2121.
- [11] S. Ghosh, K. Ganesan, S.R. Polaki, T. Ravindran, N.G. Krishna, M. Kamruddin, A. Tyagi, *J. Raman Spectrosc.* 45 (2014) 642.
- [12] J. Shena, A. Liua, Y. Tua, H. Wanga, R. Jianga, J. Ouyangc, Y. Chen, *Electrochimica Acta* 78 (2012) 122-132.
- [13] A.C. Ferrari, J. Robertson, *Philos. Trans. R. Soc. Lond. A*, 362 (2004) 2477-2512
- [14] A. Jorio, *ISRN Nanotechnology* 2012 (2012) 1-16.
- [15] S. Ghosh, K. Ganesan, S.R. Polaki, Tom Mathews, Sandip Dhara, M. Kamruddin, A. Tyagi, *Appl. Surf. Sc.* 349 (2015) 576-581.
- [16] A. Winchester, S. Ghosh, S. Feng, A.L. Elias, T. Mallouk, M. Terrones, S. Talapatra, *Appl. Mater. Interfaces* 6 (2014) 2125-2130.